Received: Added at production | Revised: Added at production | Accepted: Added at production

DOI: xxx/xxxx

RESEARCH ARTICLE

Optimal Design of Broadband NRD Guide Devices Using Binary GA and 2D-FVFEM†

Tahir Bashir[1] | Keita, Morimoto[1] | Akito Iguchi[1] | Yasuhide Tsuji*[1] | Tatsuya Kashiwa[2] | Shinji Nishiwaki[3]

[1]Information and Electronics Engineering, Muroran Institute of Technology, Muroran, Japan
[2]Information and Communication Engineering, Kitami Institute of Technology, Kitami, Japan
[3]Graduate School of Engineering, Kyoto University, Kyoto, Japan

Correspondence
*Yasuhide Tsuji Email: y-tsuji@mmm.muroran-it.ac.jp

Present Address
Muroran Institute of Technology 27-1 Mizumoto-cho, Muroran, Hokkaido, 050-8585, Japan

Summary

In this paper, a class of broadband NRD guide devices based on digital material are presented using optimal design technique. The NRD guides to be discussed here include low crosstalk crossing waveguide, T-branch, 90°-bend, and Z-bend waveguide. To reduce the computational efforts, we employ recently proposed 2D-FVFEM as simulation method. Based on digital material optimization strategy, binary GA is implemented to obtain an optimal device structure in the design region. To achieve the desired properties, we introduce a unique one-two symmetric conditions for the structural optimization. And hence, the designed crossing, T-branch, 90°-bend, and Z-bend, respectively, achieve high transmission efficiencies greater than 99.5%, 49.5%:49.5%, 99.4%, and 99.9% at operating frequency 60 GHz, and, furthermore, achieve broadband property as well in the frequency range of 58 GHz–64 GHz, 58 GHz–62 GHz, 59 GHz–62 GHz, and 59 GHz–63 GHz. The numerical results of 2D-FVFEM are also verified by 3D-FVFEM. Owing to excellent performances, the proposed NRD guide devices can be useful in a lot of millimeter-wave circuit and system applications.

KEYWORDS:
Non-radiative dielectric waveguide (NRD guide), binary genetic algorithm, full-vectorial finite element method

1 | INTRODUCTION

Development made the NRD technology matured and declared that the Non-Radiative Dielectric (NRD) waveguide is a most attractive building blocks for compact millimeter-wave circuit applications [1,2,3,4,5,6,7,8]. The NRD guide is a promising platform for millimeter-wave integrated circuits. The study, development, and design of circuit elements with various functions are not yet sufficient. After extensive research, the realization of compact circuit with non-radiative transmission and broad bandwidth is still hard due to structural and some other limitations of waveguide properties. However, NRD platform ensured all these millstones at one place such as low-cost, low radiation loss, high transmission efficiency and broad bandwidth. A few millimeter-wave circuit components based on NRD have been proposed so far, which include directional coupler, filter, circulator and antennas [9,10,11]. Still, numerous NRD guide components with different functionality have not been discussed specially at broad frequency band.

†This is an example for title footnote.

Various optimization methods have been proposed and their effectiveness has been shown. There are inherent difficulties in designing NRD guides, and it is especially important to study wideband operation. Several optimal design approaches have been proposed for optical guide devices such as geometric optimization, topology optimization, genetic algorithm, particle swarm optimization, direct binary search algorithm, inverse design algorithm, and differential evolution algorithm [12,13,14,15,16,17,18,19,20,21,22,23,24,25,26,27,28,29,30,31,32,33,34,35]. But research for the development of these optimal design approaches with different optimization strategies for NRD guide devices have not been conducted. All these above optimization approaches have good enough search ability to design NRD guides with unique structure ideas. NRD guide have a structure in which a dielectric waveguide is sandwiched between metal plates so, efficient optimization approach with high search ability is a bit challenging. NRD guide have a capability to greatly suppress the undesired radiation loss and some other discontinuities specially at sharp bend due to cut-ff property of the metal plates which are separated by less than half of the free space wavelength. NRD guide support two non-radiative orthogonal modes such as LSM_{01} and LSE_{01} and the undesired coupling of these modes at sharp bending point may effect on the performance of NRD guide devices. Therefore, an efficient optimal design approaches with best optimization strategies and interesting structural symmetric conditions are required for the designing of high performance NRD guide devices. So, this paper is mainly concerned with optimal design of boradband NRD guides which are essential for millimeter-wave applications.

The purpose of this paper is to present optimal design of broadband NRD guide devices that are useful for the development of millimeter-wave circuits. The purpose is to realize these devices using same optimization method. Therefore, designing based on digital material concept is useful, and genetic algorithm is used as an optimization method. We propose an efficient design method that uses the recently proposed 2D-FVFEM for the numerical analysis of NRD guide devices and compared it with conventionally required 3D-FEM [36,37]. Without sacrificing accuracy, 2D-FVFEM analyzes the frequency characteristics very efficiently than 3D-FEM.

In our previous studies, we considered single operating frequency in the optimal design. The obtained devices may have narrow bandwidth or may show abrupt performance deterioration at specific frequency due to resonance behavior. In order to widen the bandwidth, it may be possible to widen the bandwidth by discretizing the operating band at equal intervals and considering it in the objective function. Due to the resonant behavior, large deterioration of characteristics was sometimes seen at frequencies not considered. In order to avoid this, we have devised the setting of the objective function. Specifically, when the above method does not provide a sufficient wide band. We propose a method to randomly change the frequency to be considered in each generation of GA. The usefulness of this method has been confirmed through some design examples. In evolutionary methods such as GA, the search space becomes wider as the design variables increase. A larger number of individuals and number of iterations will be required, but in the design using this digital material, due to the non-radioactivity of the NRD guide, it is possible to design a very compact element. It is possible to efficiently optimize by GA with relatively few design variables.

2 | NRD GUIDE

NRD guide has been proposed as a millimeter waveguide by T. Yoneyama [1]. Its structure consists of a dielectric sandwiched between metal parallel plates as shown in Fig. 1(a). Structurally, it is similer to H-guide except operational principle and separation between plates which is less than $\lambda_0/2$. If the dielectric strip is placed between metal plates, the electromagnetic waves can freely propagate along strip. However, radiated waves can be suppressed by cutt-off nature of the parallel plate guide. In general, a propagation loss of millimeter wave in the metal become larger compared with that of microwave. However, in the NRD guide, the current flowing through the metal is small, and most of the electromagnetic energy flows through the dielectric. As a result, propagation loss is small.

NRD guides usually support two orthogonal modes. One is LSM_{01} mode whose electric field is parallel to the metal and the other is LSE_{01} mode whose electric field is perpendicular to the metal. Fig. 1(b) shows the filed lines of LSM_{01} and LSE_{01} mode. Both modes are non-radiative in nature and cannot propagate within air region sandwiched metal parallel plates and can be used as a non-radiative waveguide. LSM_{01} mode whose polarization is parallel to the metal is usually used in NRD guide, in contrasted to microstrip line which supports polarization perpendicular to the metal. Furthermore, the dispersion relation of NRD guide is also calculated as shown in Fig. 1(c).

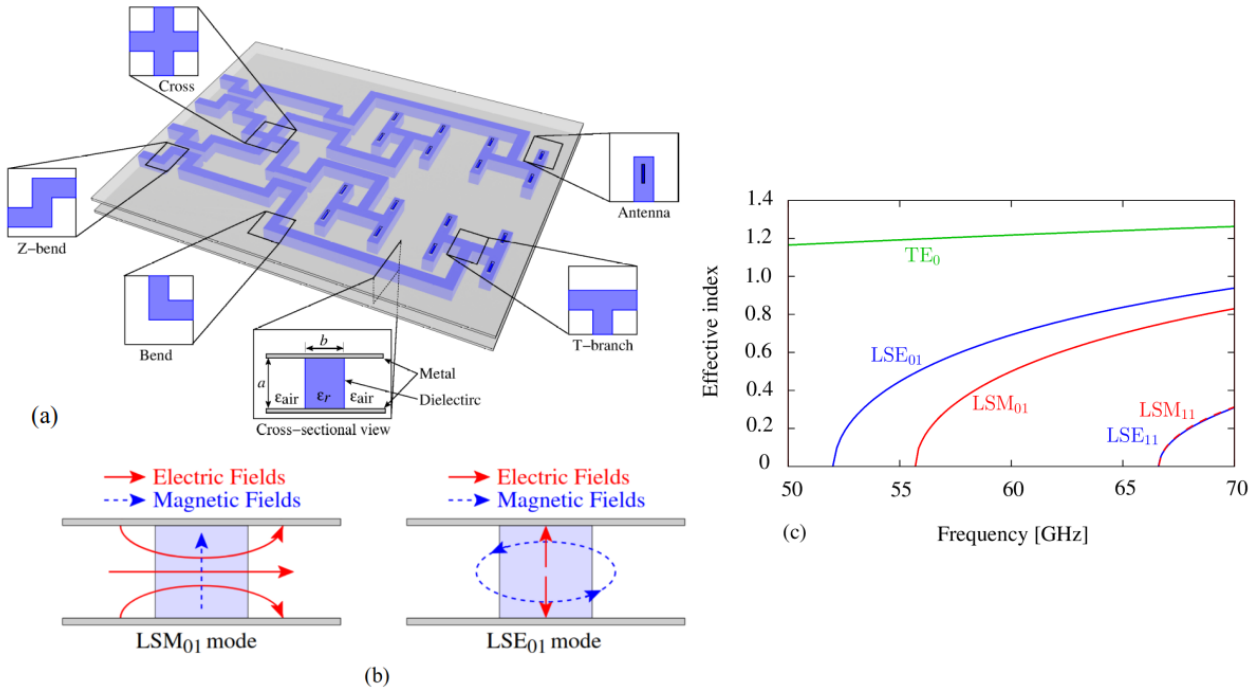

FIGURE 1 NRD guide (a) an image of NRD integrated circuit, (b) propagating modes, (c) dispersion relation $a = 2.25$ mm, $b = 2$ mm, $\epsilon_r = 2.2$

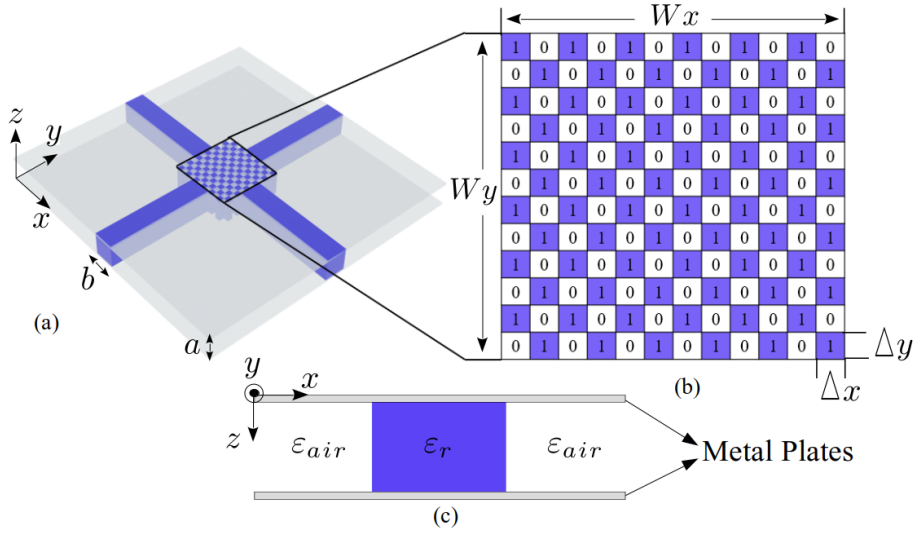

FIGURE 2 Non-radiative dielectric (NRD) waveguide (a) design setup (b) optimization strategy (c) front view of NRD guide

3 | BINARY GENETIC ALGORITHM

3.1 | Optimization Strategy

In order to optimize the design region of the proposed NRD guide devices we implement binary GA using digital material optimization strategy when fundamental LSM_{01} mode is launched at port 1. We used several numerical design variables to express the design region that are optimized. First, design region is discretized into grid pattern as shown in Fig. 2 and each block of the pattern called pixel have a material either dielectric or air in the form of 1 and 0 known as digital material concept. Our optimal design approach optimizes the pattern by assigning material to each pixel and obtain a mosaic like structure that

satisfy the desired properties in conclusion.

In order to realize the high-performance millimeter-wave circuit, we designed several compact NRD circuit components having high transmission efficiency and broad bandwidth capability using efficient optimization method. The number of mosaics is the design freedom of our optimization method. A large number of mosaics may require large population size and number of iterations that may degrade the design efficiency of optimization method. For the realization of highly attributed circuit components, we used suitable mosaic size that is completely compatible with the design efficiency of optimization method. Implementation of algorithm and optimization results of the proposed NRD guide devices are discussed below.

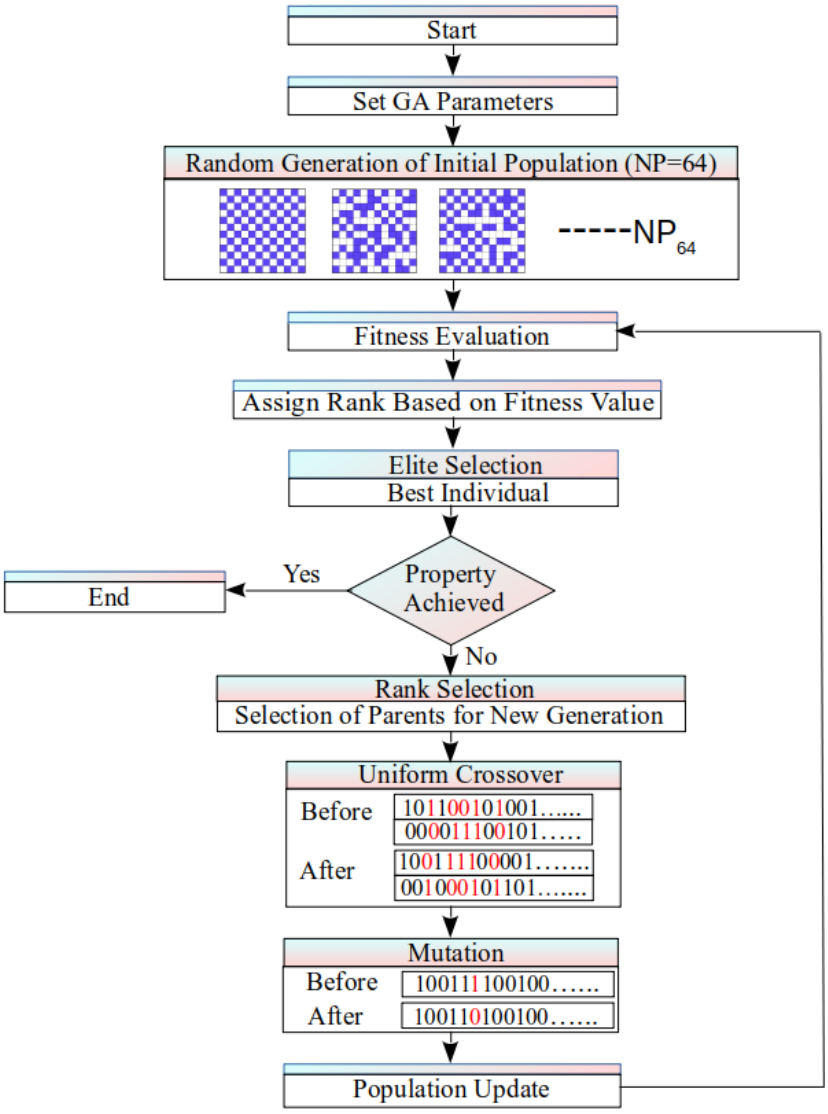

FIGURE 3 Working procedure of binary GA

3.2 | Implementation of Algorithm

Binary GA is a stochastic based search algorithm called evolutionary computation. The search procedure of binary GA is similar to Charles Darwin theory of evolution. For more clarification, the implementation and search procedure of algorithm is presented in the flowchart of binary GA as shown in Fig. 3. The random generation of the initial population is the first step

in GA optimization. It should be emphasized that a large population slows down the optimization process, whereas a small population may not be suitable for a mating pool. As a result, multiple trials are required to determine the appropriate size. In this optimization method, the size of the randomly generated population is 64. To optimize the design region of the NRD guide, a random population is formed that has a set of individuals, also known as chromosomes, encoded by digital technique. Each individual is a mosaic-like structure made up of a set of pixels (called a gene) arranged in the form of 1 and 0. After the population is randomly generated, the problem-dependent fitness function calculate each individual quality (called fitness value) and then assigns a rank to each individual based on the fitness value. The population is then evolved utilizing three biologically inspired operators, such as selection, crossover, and mutation, using binary GA.

Selection is a procedure to update the generation by replacing the highly fit individuals with previous ones those are poor in fitness value. Individuals are selected for later mating through crossover and mutation in the first stage of evolution. From many types of selections schemes, we considered two of them in our study. To begin, we employed elite selection to save the best individual from the entire population. On other hand, rank selection chooses the best individuals from population for crossover purpose.

Crossover is a significant part of GA, in which two individuals mate and exchange some bits to create a new individual with some attributes that are identical to the parents. Our optimal design approach used uniform crossover technique in which each pixel is randomly chosen from one of the corresponding pixels of the parent individuals.

Mutation is a third operator in evolutionary process of GA that is used to maintain the genetic diversity from one population to the next and to avoid local minima by preventing population of individuals from becoming too similar. There are several types of mutation operators, but we utilized the simplest one, bit flip mutation. A bit flip mutant is the inverting of bits according to a preset probability to create a unique individual. In this optimization approach, the mutation rate is 0.05. Now the evolution of randomly generated population has finished. This search process is repeated until the completion of pre-defined number of generations. Finally, the best individual at last generation will be optimum mosaic-like structure of NRD guide.

4 | DESIGN EXAMPLE OF NRD GUIDE DEVICES

In this paper, we proposed four NRD guide devices. The gap between metal plates is $a = 2.25$ mm, width of the dielectric strip is $b = 2$ mm, and the permittivity of dielectric and air is $\varepsilon_r = 2.2$, $\varepsilon_{\text{air}} = 1$ respectively. In addition, we considered LSM_{01} mode for port 1 incident.

4.1 | Crossing Waveguide

First, we design a low crosstalk NRD crossing waveguide whose initial design model is shown in Fig. 4(a). The configurational parameters of the design setup are chosen to be $d = 5$ mm, $l = 10$ mm, and $W_x = W_y = 6$ mm. The design region is discretized into 144 pixels and the footprint of each pixel is set to be 0.5 mm $\times$ 0.5 mm that is quarter of the dielectric strip width $b = 2$ mm. In order to make the fabrication feasible, the pixel size is determined by considering the operating wavelength, guide width, and fabrication sensitivity. Applying unique one-two symmetric conditions, the pixels in half of the design region indicated by red line are designed as shown in Figure 4(a). In order to maximize the output power at frequency 60 GHz, we define the objective function as follow. The figure of merit for this device is maximum transmission efficiency at output port 3 when LSM_{01} mode at 60 GHz is launched into input port 1.

$$\text{Minimize } C = 1 - |S_{31}|^2 \qquad \text{(at 60 GHz)} \tag{1}$$

Furthermore, we achieved a broadband property in NRD crossing waveguide by using objective function as follow.

$$\text{Minimize } C = \sum_{i=1}^{3} (1 - |S_{31}(f_i)|^2) \tag{2}$$

$$(f_{1,2,3} = 58, 60, 62 \text{ GHz})$$

The optimized structures and prpagation fields of both NRD crossing waveguides are shown in Fig. 4 and Fig. 5 respectively. The NRD crossing guide at frequency 60 GHz achieved a high transmission power $|S_{31}|^2 = 0.995$ as shown in Fig. 6(a). The frequency characteristics shows that the crossing guide achieved almost ideal bandwidth property from 58 GHz-64 GHz as

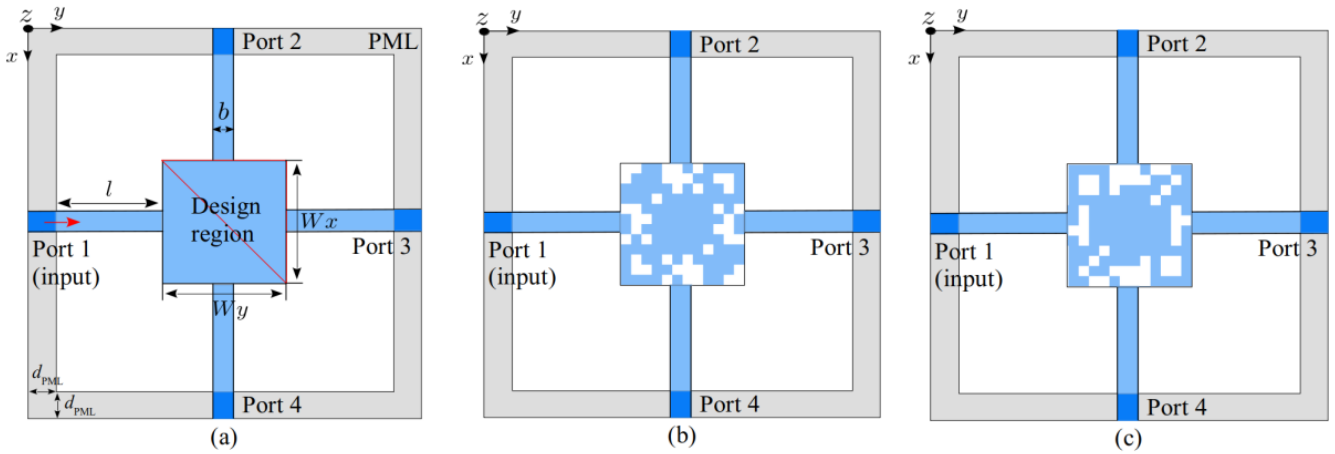

FIGURE 4 NRD crossing waveguide (a) initial design model (b) optimized structure at 60GHz and (c) optimized structure for broadband operation

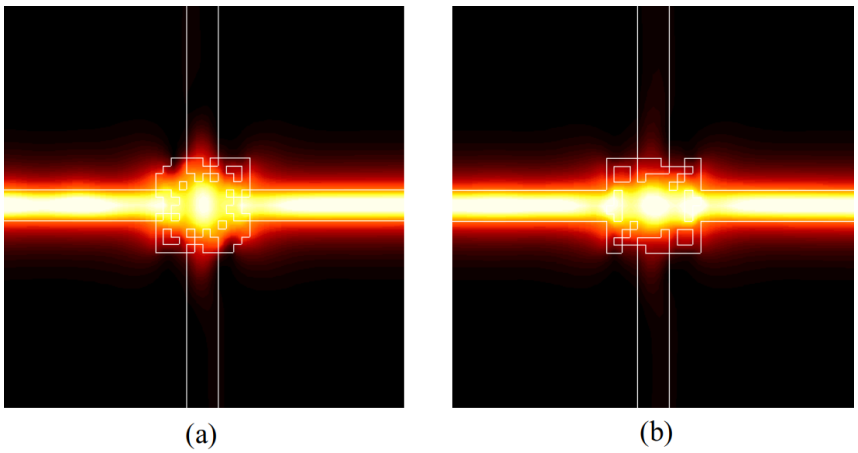

FIGURE 5 Propagation fields of NRD crossing waveguides (a) at operating frequency 60 GHz (b) broadband crossing guide at 60 GHz

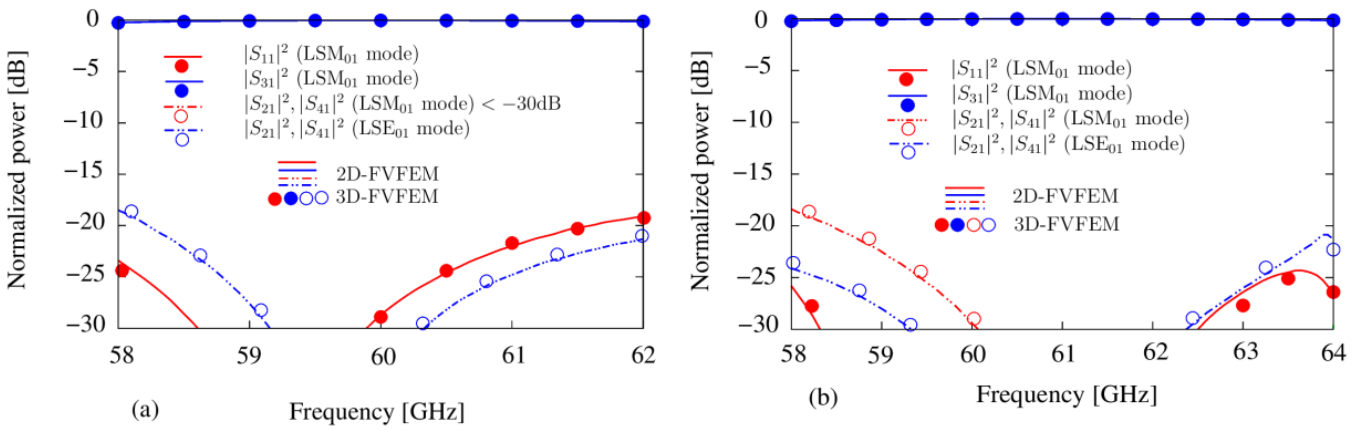

FIGURE 6 Frequency characteristics of NRD crossing waveguide (a) at operating frequency 60 GHz (b) broadband operation

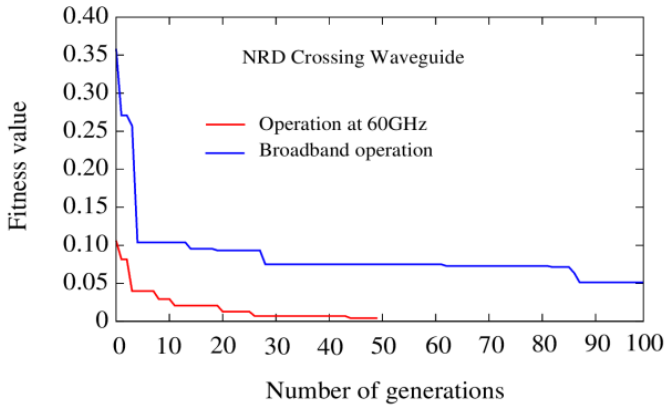

FIGURE 7 Convergence of NRD crossing waveguide

shown in Fig. 6(b). In Fig. 6, the frequency charactristics of devices designed by 2D-FVFEM are also verified by 3D-FVFEM. The fitness value as a function of the number of generations is shown in Fig. 7. The optimal design approach converge the solution very efficiently for both NRD guide devices in just 50 and 100 number of generations. We can see that design efficiency is greatly improved by using 2D-FVFEM. The 2D-FVFEM analysis used only 2.7 s with 0.26 GB of memory for computation at PC Intel(R) Core(TM) i9-9900k CPU at 3.60 GHz, whereas 3D-FVFEM required 798 s with 0.92 GB of memory using a PC Intel(R) Xeon (R) Gold 6242 CPU at 2.80 GHz.

4.1.1 | T-branch

Now, we design a NRD T-branch guide which split the input power equally into output ports. The initial design setup of T-branch guide is shown in Fig. 8(a). The configurational parameters are same as considered in crossing guide except symmetric conditions. In this example, we considered one-two symmetric condition in rectangle form for equal and smooth distribution of power towards output ports as shown in Fig. 8(a). Due to considered symmetry, 72 pixels ($N_x = 12$ $N_y = 6$ mm) in the upper half of the design region are optimized. To achieve the maximum transmission at 60 GHz, we considered the following objective function.

$$\text{Minimize } C = 1 - |S_{21}|^2 - |S_{41}|^2 \qquad \text{(at 60 GHz)} \tag{3}$$

Whereas, $|S_{21}|^2$ and $|S_{41}|^2$ are output powers at port 2 and port 4 respectively. In addition, we used a following objective function for broadband operation of NRD T-branch waveguide.

$$\text{Minimize } C = \sum_{i=1}^{5} (1 - |S_{21}(f_i)|^2 - |S_{41}(f_i)|^2) \tag{4}$$

$$(f_{1,2,3,4,5} = 58, 59, 60, 61, 62 \text{ GHz})$$

The optimized structures of T-branch guides are shown in Fig. 8. To optimize the structure which split the maximum power equally with smooth propagation behavior is a bit difficult in case of NRD T-branch guide, but in our study, we can see that how incident power smoothly split into two output ports in both cases as shown in Fig. 9. The normalized splitting power ratio of NRD T-branch guide at 60 GHz is $|S_{21}|^2 = 0.495$ $|S_{41}|^2 = 0.495$ as shown in Fig. 10(a). Fig. 10(b) shows that the proposed T-branch guide achieved broad bandwidth in the frequency range of 58 GHz-62 GHz. However, it shows a negligible reflection $|S_{11}|^2$ at 58 GHz or 62 GHz because of structural limitations. The value of fitness function versus number of generations are shown in Fig. 11. It clearly shows that the solution of T-branch guide at frequency 60 GHz is quickly converged within 50 generations but broadband operation is quite differ due to multiple frequencies involve during simulations. We achieved good enough convergence with desired broadband property in 300 generations. However, more than this takes a long computational time and the solution will not more converge as shown in Fig. 11.

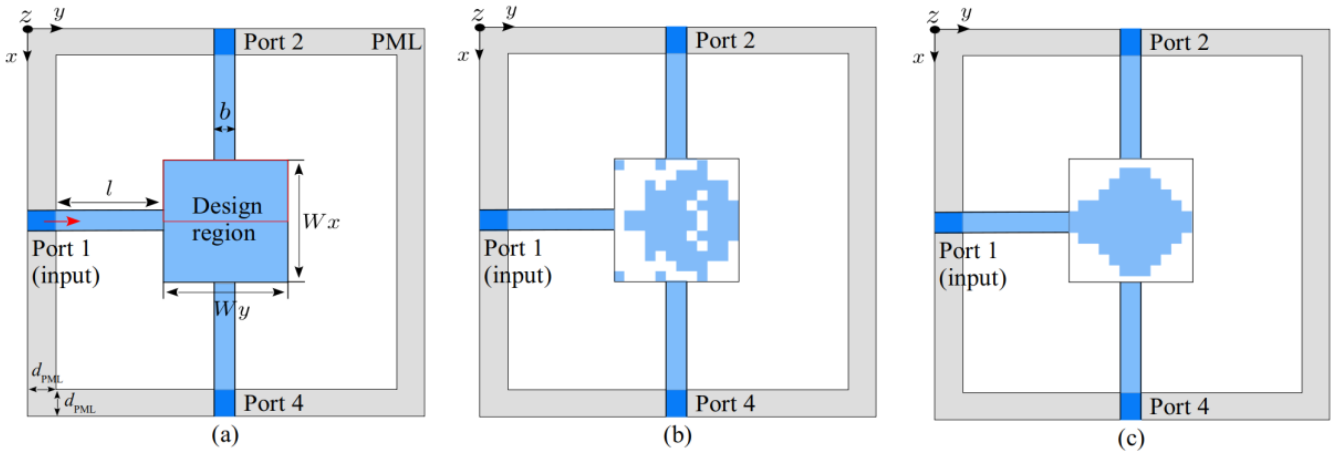

FIGURE 8 NRD T-branch waveguide (a) initial design model (b) optimized structure at 60GHz and (c) optimized structure for broadband operation

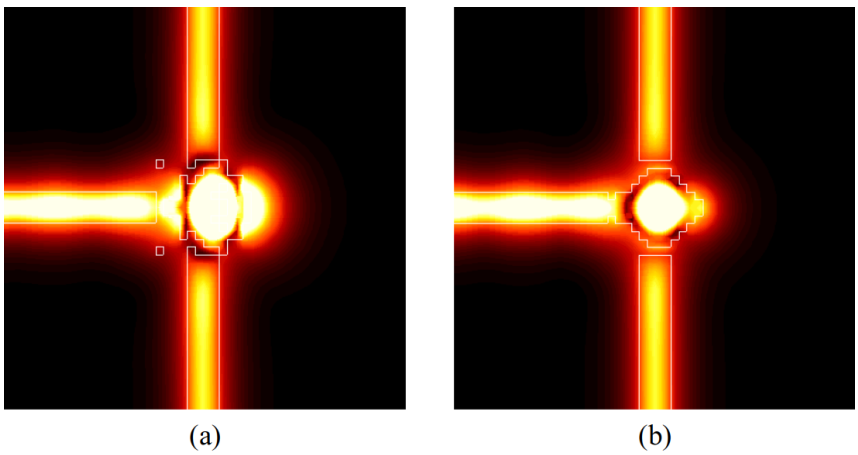

FIGURE 9 Propagation fields of NRD T-branch waveguides (a) at operating frequency 60 GHz (b) broadband T-branch guide at 60 GHz

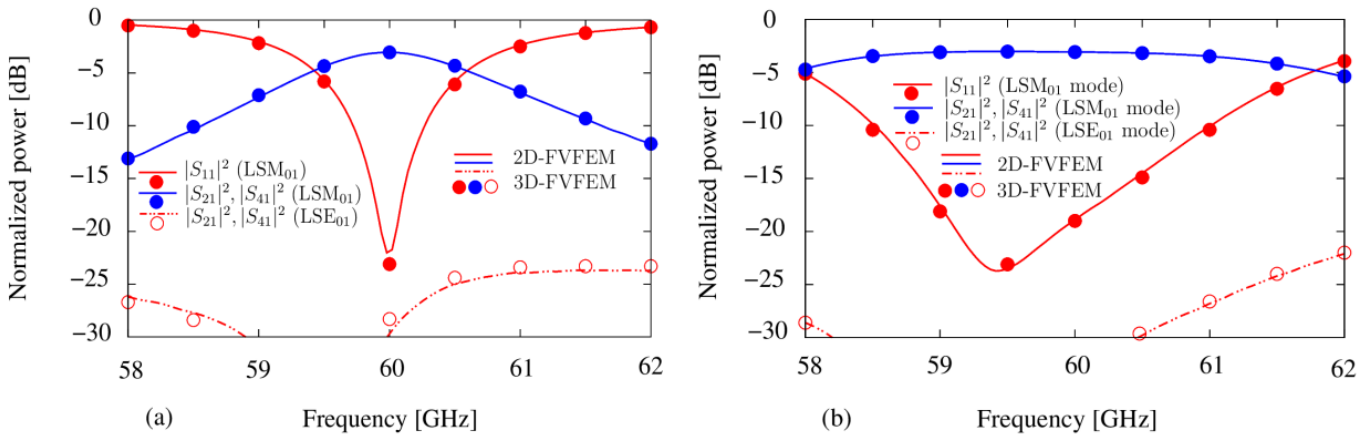

FIGURE 10 Frequency characteristics of NRD T-branch waveguide (a) at operating frequency 60 GHz (b) broadband operation

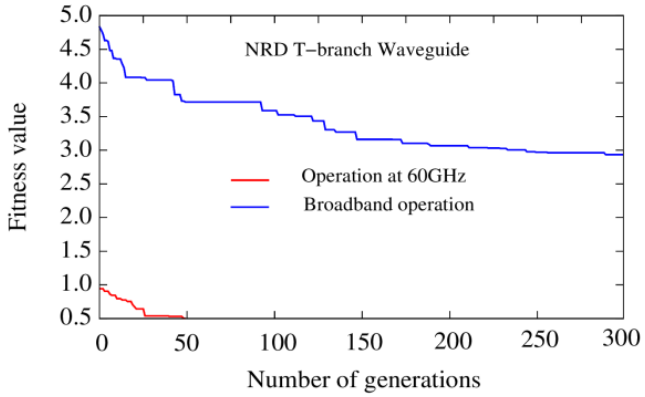

FIGURE 11 Convergence of NRD T-branch waveguide

4.1.2 | 90°-bend

Next, NRD 90°-bend is optimized whose initial design structure is shown in Fig. 12(a). The geometrical parameters, port of incident, number of pixels to be optimized and symmetric conditions are same as considered in previous example of crossing waveguide. The optimized structure and propagation fields are shown in Fig. 12 and 13. The objective functions of 90°-bend are given below. However, to achieve the broad bandwidth of 90°-bend is quite hard due to sharp bending structure.

$$\text{Minimize } C = 1 - |S_{21}|^2 \qquad \text{(at 60 GHz)} \tag{5}$$

$$\text{Minimize } C = \sum_{i=1}^{3} (1 - |S_{21}(f_i)|^2) \tag{6}$$
$$(f_{1,2,3} = 59, 60, 61 \text{ GHz})$$

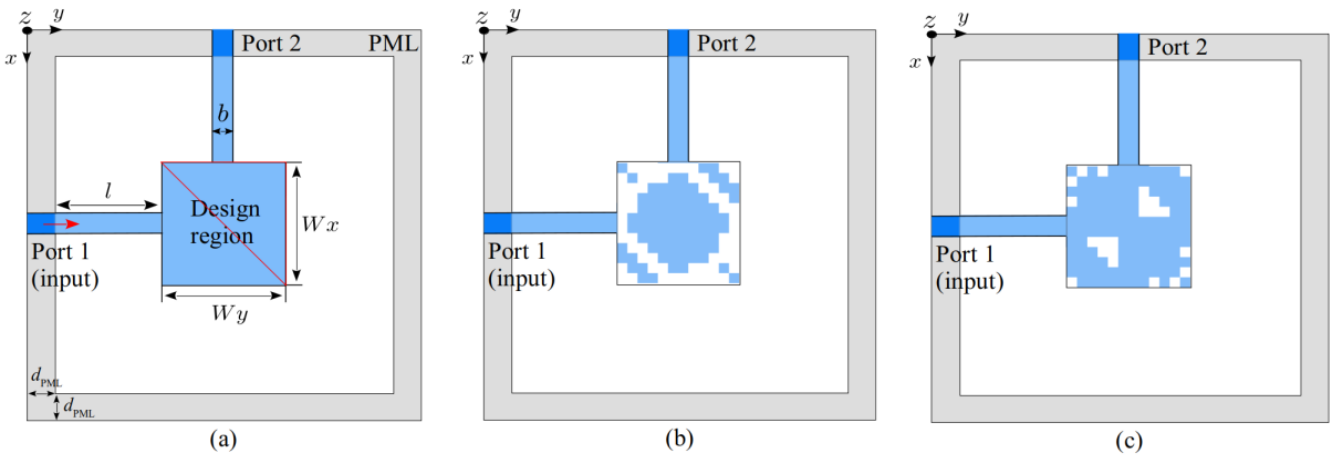

FIGURE 12 NRD 90°-bend waveguide (a) initial design model (b) optimized structure at 60GHz and (c) optimized structure for broadband operation

The structure of 90°-bend at 60 GHz and at broadband operation are successfully optimized in 50 and 200 generations respectively shown in Fig. 15. The normalized transmission power $|S_{21}|^2$ at 60 GHz is 0.994 as shown in Fig. 14(a). The frequency characteristics of broadband 90°-bend is shown in Fig. 14(b) and it achieves a good enough bandwidth around 2.3 GHz. However, its comparatively less than other devices because it shows a small but considerable reflection power $|S_{11}|^2$ at 59 GHz

and 62 GHz due to sharp bend. To achieve the desired properties especially high bandwidth, a more sensitive optimal design approach is required for the design of 90°-bend waveguide.

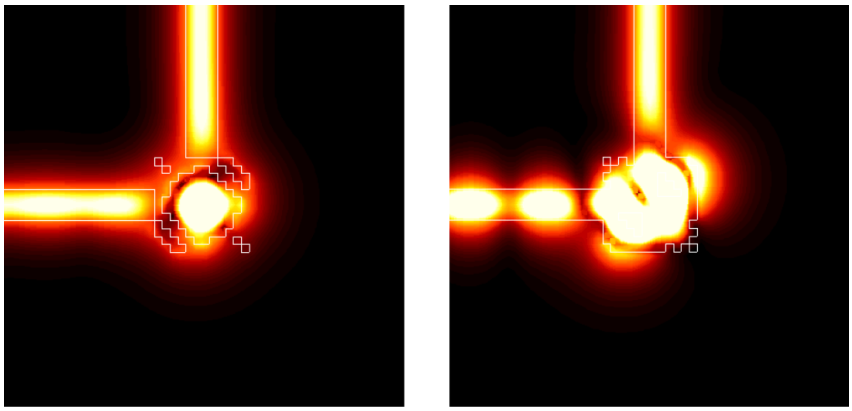

FIGURE 13 Propagation fields of NRD 90°-bend waveguides (a) at operating frequency 60 GHz (b) broadband T-branch guide at 60 GHz

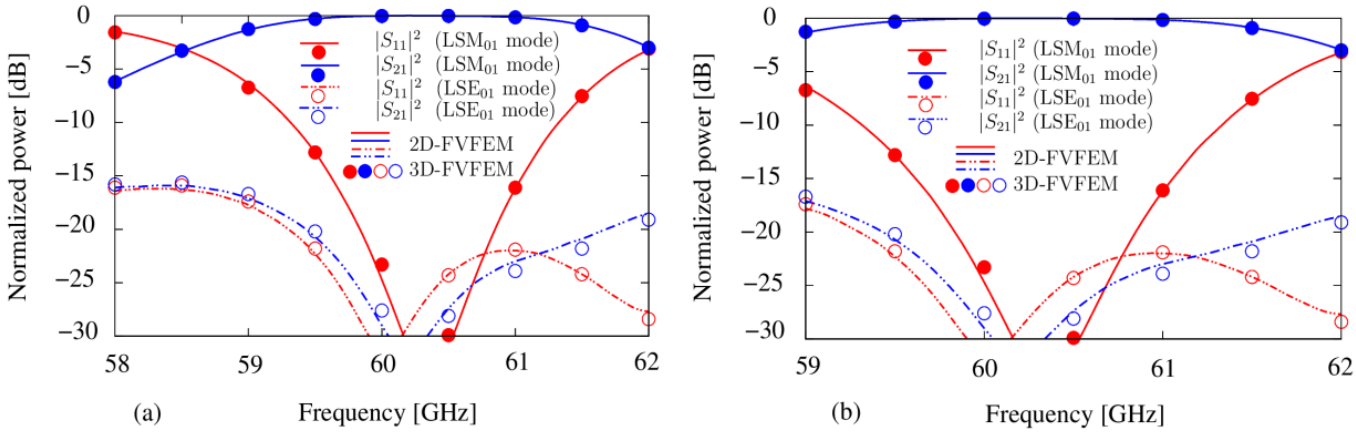

FIGURE 14 Frequency characteristics of NRD 90°-bend waveguide (a) at operating frequency 60 GHz (b) broadband operation

4.1.3 | Z-bend

Finally, NRD Z-bend guide is designed whose initial model is shown in Fig. 16(a). The symmetric conditions and structural parameters of this model are exactly same as in previous example except size of the design region as follows: $W_x = 10$ mm, $W_y = 6$ mm. We assume half of the design region for the optimization of pixels as shown in Fig 16(a). To maximize the power of LSM$_{01}$ mode at frequency 60 GHz, we used the following objective function.

$$\text{Minimize } C = 1 - |S_{21}|^2 \quad \text{(at 60 GHz)} \tag{7}$$

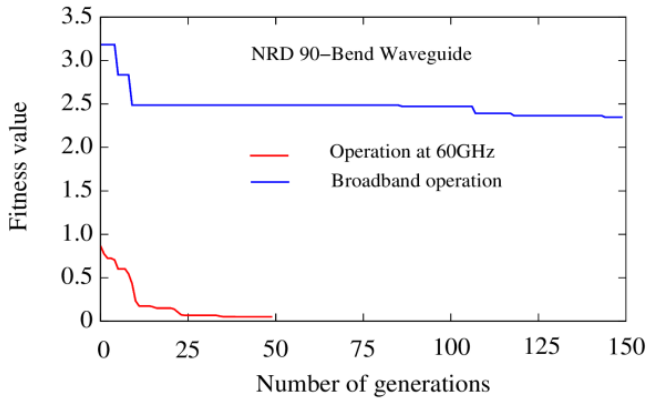

FIGURE 15 Convergence of NRD 90°-bend waveguide

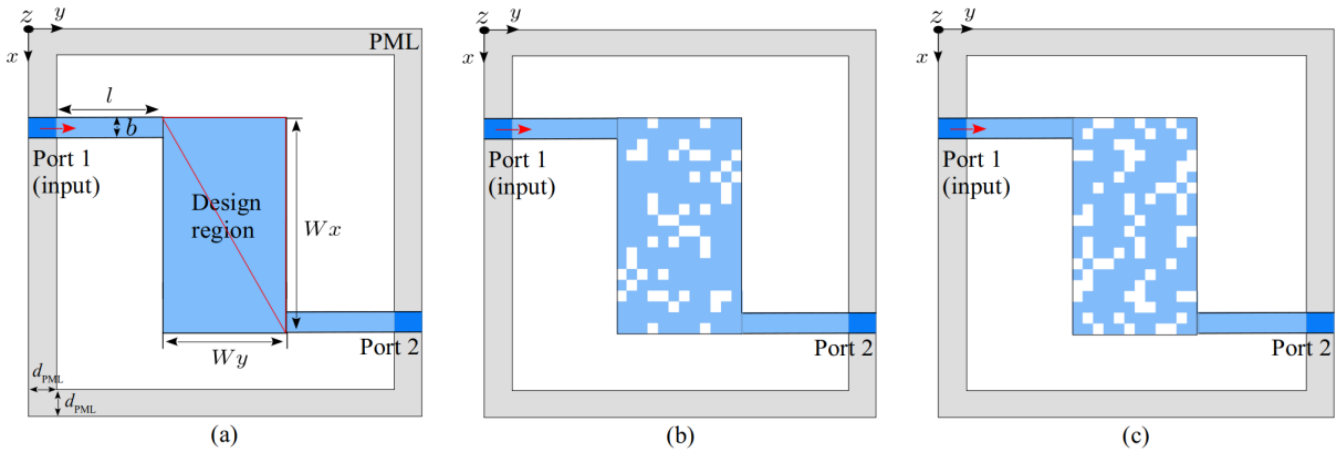

FIGURE 16 NRD Z-bend waveguide (a) initial design model (b) optimized structure at 60GHz and (c) optimized structure for broadband operation

In order to achieve the broadband property more stably we proposed an interesting objective function as given below. The proposed objective function is more general one and not limited to the design of Z-bend guide. To compute the random frequency, we used a random function to select a number between 0 and 1 and RND_{MAX} function is also used for the normalization.

$$\begin{gathered} \text{Minimize } C = 1 - |S_{21}(f)|^2 \\ f = f_{\min} + (f_{\max} - f_{\min}) \times \text{random}()/\text{RND}_{\text{MAX}} \\ (f_{\min} = 59 \text{ GHz},\ f_{\max} = 62 \text{ GHz}) \end{gathered} \tag{8}$$

The proposed objective function randomly selects the frequency in the range of 59 GHz to 62 GHz for each generation of GA to avoid degradation of device performance at unconsidered frequency. Using this function, we achieved almost ideal broadband property from 59 GHz-63 GHz as shown in Fig. 18(b). The considered objective function does not guarantee to achieve broad bandwidth for other NRD guides but in case of Z-bend its functioning well. The optimized structures and propagation fields of both Z-bend devices are shown in Fig. 16 and Fig. 17 respectively. The normalized power is $|S_{21}|^2 = 0.999$ at operating frequency 60 GHz as shown in Fig. 18(a). Fig. 19 shows the calculated results of considered objective functions in term of minimum fitness value at different frequencies. Due to simple in structure Z-bend guide at 60 GHz converge very smoothly even from starting to the completion of generations.

However, in case of broadband operation, it shows the abrupt changes in fitness values along number of generation due to random selection of frequencies in the range of 59 GHz to 62 GHz as shown in Fig. 19. We can see that in Fig. 19 the convergence

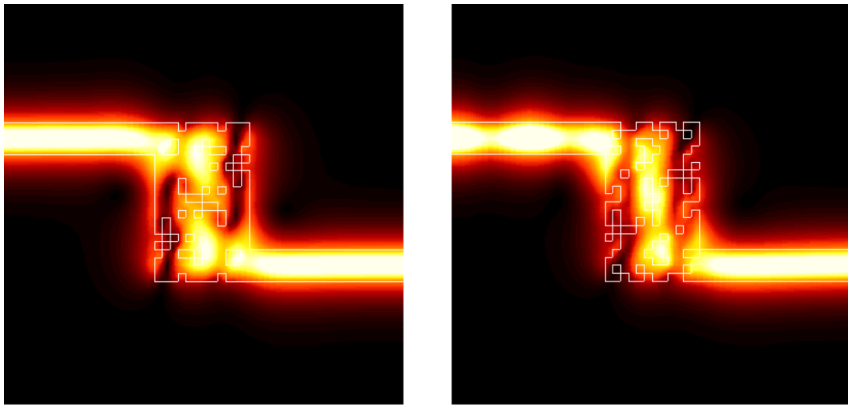

FIGURE 17 Propagation fields of NRD Z-bend waveguides (a) at operating frequency 60 GHz (b) broadband Z-bend guide at 60 GHz

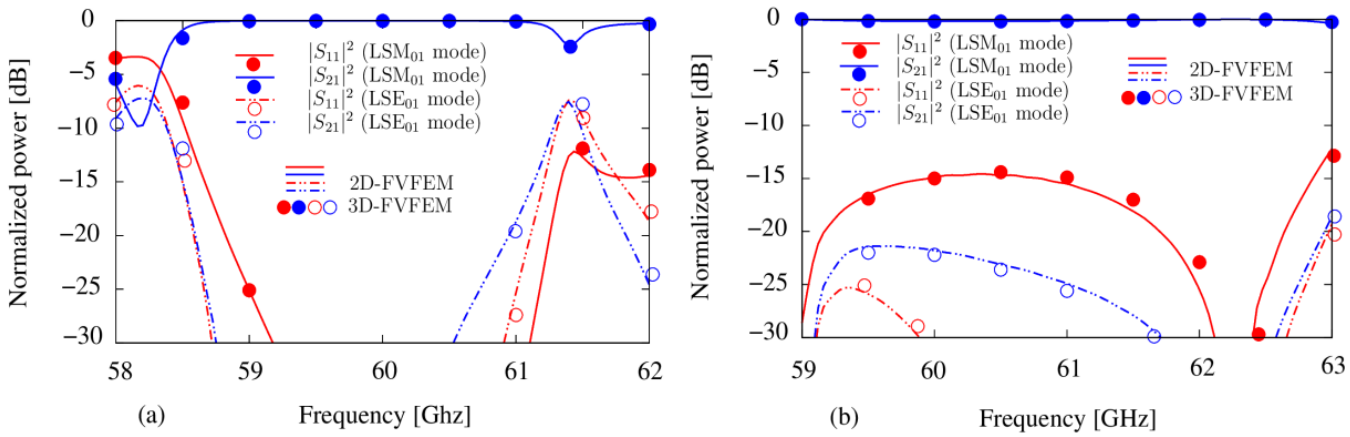

FIGURE 18 Frequency characteristics of NRD Z-bend waveguide (a) at operating frequency 60 GHz (b) broadband operation

TABLE 1 Performance analysis of the proposed NRD guide devices

NRD Guides	Transmission [dB]		Reflection [dB]		Bandwidth
Performance	LSM_{01}	LSE_{01}	LSM_{01}	LSE_{01}	[GHz]
Crossing	−0.01	−40.0	−30.0	−33.9	6.0
T-branch	−3.05	−30.0	−22.2	−60.0	4.0
90°-bend	−0.02	−29.2	−25.2	−31.5	2.3
Z-bend	−0.001	−41.5	−53.9	−40.0	4.0

is almost same from 40 number of generations to till 85 although frequencies are different. So, to increase the generations will be not efective except consumption of time because it will show the same convergence behavior except some particlar frequency points. Furthermore, the performance detail of proposed NRD guides is summerized in Table. 1.

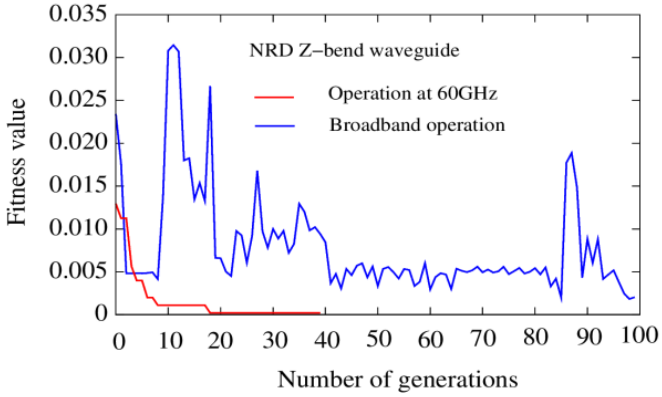

FIGURE 19 Convergence of NRD Z-bend waveguide

5 | CONCLUSION

In summary, we developed efficient optimal design strategy of broadband NRD guide devices based on digital material. To minimize the computational cost, we used originally developed 2D-FVFEM for the numerical simulation of these devices. This method can be applied to the design of THz waveguide devices with a similar structure, but caution is required in the frequency band where conductor loss cannot be ignored. Binary GA based on digital material strategy is implemented for the optimization of proposed NRD guide devices. A unique one-two symmetric condition is imposed in the design region to achieve the desired properties. The designed crossing, T-branch, 90°-bend, and Z-bend, respectively, achieve high transmission efficiencies greater than 99.5%, 49.5%:49.5%, 99.4%, and 99.9% at operating frequency 60 GHz, and the achieve broad bandwidth around 6 GHz, 4 GHz, 2.3 GHz, and 4 GHz. In our study, we confirmed the realization of several kinds of high performance NRD guide devices under the same design strategy. Furthermore, the numerical results of 2D-FVFEM are also verified by 3D-FVFEM.

ACKNOWLEDGMENTS

This work was supported by JSPS (Japan) KAKENHI Grant Number 18K04276.

Conflict of interest

The authors declare no conflicts of interest.

References

1. Yoneyama T, Nishida S. Nonradiative Dielectric Waveguide for Millimeter-Wave Integrated Circuits. *IEEE Transactions on Microwave Theory and Techniques* 1981; 29(11): 1188-1192. doi: 10.1109/TMTT.1981.1130529

2. Yoneyama T. Recent development in NRD-guide technology. *In Annales des télécommunications* 1992; 47(11): 508-514. doi: 10.1007/BF02998313

3. Xu F, Wu K. Substrate Integrated Nonradiative Dielectric Waveguide Structures Directly Fabricated on Printed Circuit Boards and Metallized Dielectric Layers. *IEEE Transactions on Microwave Theory and Techniques* 2011; 59(12): 3076-3086. doi: 10.1109/TMTT.2011.2168969

4. Yoneyama T, Tozawa N, Nishida S. Loss Measurements of Nonradiative Dielectric Waveguide (Special Papers). *IEEE Transactions on Microwave Theory and Techniques* 1984; 32(8): 943-946. doi: 10.1109/TMTT.1984.1132804

5. Yoneyama T, Tamaki H, Nishida S. Analysis and Measurements of Nonradiative Dielectric Waveguide Bends. *IEEE Transactions on Microwave Theory and Techniques* 1986; 34(8): 876-882. doi: 10.1109/TMTT.1986.1133460

6. Maamria K, Wagatsuma T, Yoneyama T. Leaky NRD guide as a feeder for microwave planar antennas. *IEEE Transactions on Antennas and Propagation* 1993; 41(12): 1680-1686. doi: 10.1109/8.273312

7. Wu K. A combined efficient approach for analysis of nonradiative dielectric (NRD) waveguide components. *IEEE Transactions on Microwave Theory and Techniques* 1994; 42(4): 672-677. doi: 10.1109/22.285075

8. Huang J, Wu K, Kuroki F, Yoneyama T. Computer-aided design and optimization of NRD-guide mode suppressors. *IEEE Transactions on Microwave Theory and Techniques* 1996; 44(6): 905-910. doi: 10.1109/22.506450

9. Dallaire J, Wu K. Complete characterization of transmission losses in generalized nonradiative dielectric (NRD) waveguide. *IEEE Transactions on Microwave Theory and Techniques* 2000; 48(1): 121-125. doi: 10.1109/22.817480

10. Ye L, Zhang Y, Xu R, Lin W. A terahertz broadband 3dB directional coupler based on bridged PPDW. *Opt. Express* 2011; 19(20): 18910–18916. doi: 10.1364/OE.19.018910

11. Schmid U, Menzel W. A 24 GHz microstrip antenna array with a non-radiative dielectric waveguide (NRD-guide) feeding network. *11th International Symposium on Antenna Technology and Applied Electromagnetics [ANTEM 2005]* 2005: 1-4. doi: 10.1109/ANTEM.2005.7852158

12. Yoneyama T. Millimeter wave integrated circuits using nonradiative dielectric waveguide. *IEICE Trans. Electronics. (Japanese Edition)* 1990; 73(2): 87-94.

13. Rodrigues JR, Almeida VR. Geometric optimization of radiation pressure in dielectric waveguides. *OSA Continuum* 2019; 2(4): 1188–1197. doi: 10.1364/OSAC.2.001188

14. Byun JK, Park IH. Design of Dielectric Waveguide Filters Using Topology Optimization Technique. *IEEE Transactions on Magnetics* 2007; 43(4): 1573-1576. doi: 10.1109/TMAG.2007.892474

15. Jung JH. Optimal Design of Dielectric-loaded Surface Plasmon Polariton Waveguide with Genetic Algorithm. *J. Opt. Soc. Korea* 2010; 14(3): 277–281.

16. Kaliberda ME, Pogarsky SA, Kaliberda LM. SLL Reduction in Planar Dielectric Waveguide with Graphene Strips Using Genetic Algorithm. *2021 15th European Conference on Antennas and Propagation (EuCAP)* 2021: 1-5. doi: 10.23919/EuCAP51087.2021.9411043

17. Petrescu C, Ferariu L. Mode Analysis In Planar Dielectric-Conductor Waveguides Using Genetic Algorithms. *2020 International Conference and Exposition on Electrical And Power Engineering (EPE)* 2020: 259-264. doi: 10.1109/EPE50722.2020.9305568

18. Shiratori R, Nakata M, Hayashi K, Baba T. Particle swarm optimization of silicon photonic crystal waveguide transition. *Opt. Lett.* 2021; 46(8): 1904–1907. doi: 10.1364/OL.422551

19. Avad J, Demirtaş M, Perkgöz NK, Ay F. A realistic approach for designing a single-mode Y-branch for weakly guiding material system using particle swarm algorithm. *Optical and Quantum Electronics* 2020; 52: 1-10.

20. Marcuse D. Length optimization of an S-shaped transition between offset optical waveguides. *Appl. Opt.* 1978; 17(5): 763–768. doi: 10.1364/AO.17.000763

21. Wang P, Menon R. Optimization of generalized dielectric nanostructures for enhanced light trapping in thin-film photovoltaics via boosting the local density of optical states. *Opt. Express* 2014; 22(S1): A99–A110. doi: 10.1364/OE.22.000A99

22. Pan C, Liu Z, Pang Y, et al. Design of a high-performance in-coupling grating using differential evolution algorithm for waveguide display. *Opt. Express* 2018; 26(20): 26646–26662. doi: 10.1364/OE.26.026646

23. Sanchis L, Hakansson A, López-Zanón D, Bravo-Abad J, Sánchez-Dehesa J. Integrated optical devices design by genetic algorithm. *Applied Optics* 2004; 84(22): 4460-4462. doi: 10.1063/1.1738931

24. Jafar-Zanjani S, Inampudi S, Mosallaei H. Adaptive Genetic Algorithm for Optical Metasurfaces Design. *Scientific Reports* 2018; 8(1): 11040. doi: 10.1038/s41598-018-29275-z

25. Sanchis P, Villalba P, Cuesta F, et al. Highly efficient crossing structure for silicon-on-insulator waveguides. *Opt. Lett.* 2009; 34(18): 2760–2762. doi: 10.1364/OL.34.002760

26. Coccioli R, Pelosi G, Selleri S. Optimization of bends in rectangular waveguide by a finite-element genetic-algorithm procedure. *Microwave and Optical Technology Letters* 1998; 16(5): 287-290. doi: 10.1002/(SICI)1098-2760(19971205)16:5<287::AID-MOP6>3.0.CO;2-B

27. Iguchi A, Tsuji Y, Yasui T, Hirayama K. Efficient topology optimization of optical waveguide devices utilizing semi-vectorial finite-difference beam propagation method. *Opt. Express* 2017; 25(23): 28210–28222. doi: 10.1364/OE.25.028210

28. Iguchi A, Tsuji Y, Yasui T, Hirayama K. Topology Optimization of Optical Waveguide Devices Based on Beam Propagation Method With Sensitivity Analysis. *Journal of Lightwave Technology* 2016; 34(18): 4214-4220. doi: 10.1109/JLT.2016.2597308

29. Iguchi A, Tsuji Y, Yasui T, Hirayama K. Efficient Shape and Topology Optimization Based on Sensitivity Analysis for Optical Waveguide Devices Utilizing Full-Vectorial BPM. *Journal of Lightwave Technology* 2020; 38(8): 2328-2335. doi: 10.1109/JLT.2020.2964781

30. Panduro MA, Brizuela CA. A comparative analysis of the performance of GA, PSO and DE for circular antenna arrays. *2009 IEEE Antennas and Propagation Society International Symposium* 2009: 1-4. doi: 10.1109/APS.2009.5171514

31. Panduro MA. Design of coherently radiating structures in a linear array geometry using genetic algorithms. *AEU - International Journal of Electronics and Communications* 2007; 61(8): 515-520. doi: https://doi.org/10.1016/j.aeue.2006.09.002

32. Jung J. Optimal design of plasmonic waveguide using multiobjective genetic algorithm. *Optical Engineering* 2016; 55(1): 1 – 5. doi: 10.1117/1.OE.55.1.017103

33. Fu P, Shu-Cheng L, Po-Cheng T, Kuang L, Pei-Kuen W. Optimization for Gold Nanostructure-Based Surface Plasmon Biosensors Using a Microgenetic Algorithm. *ACS Photonics* 2018; 5(6): 2320-2327. doi: 10.1021/acsphotonics.8b00136

34. Jiang J, Cai J, Nordin GP, Li L. Parallel microgenetic algorithm design for photonic crystal and waveguide structures. *Opt. Lett.* 2003; 28(23): 2381–2383. doi: 10.1364/OL.28.002381

35. Nordin GP, Jiang J, Kim S, Cai J. Microgenetic-algorithm-based design of combined conventional waveguide and photonic crystal devices. In: Adibi A, Scherer A, Lin SY., eds. *Photonic Crystal Materials and Devices*. 5000. International Society for Optics and Photonics. SPIE; 2003: 152 – 160

36. Tsuji Y, Morimoto K, Iguchi A, Kashiwa T, Nishiwaki S. Two-Dimensional Full-Vectorial Finite Element Analysis of NRD Guide Devices. *IEEE Microwave and Wireless Components Letters* 2021; 31(4): 345-348. doi: 10.1109/LMWC.2021.3060179

37. Bashir T, Morimoto K, Iguchi A, Tsuji Y, Kashiwa T, Nishiwaki S. Optimal Design of NRD Guide Devices Using 2D Full-Vectorial Finite Element Method. *IEICE Electronics Express* 2021; 18(15): 1-4. doi: 10.1587/elex.18.20210243

How to cite this article: Bashir T, Morimoto K, Tsuji Y, Iguchi A, Kashiwa T, and Nishiwaki S., Optimal Design of Broadband NRD Guide Devices Using Binary GA and 2D-FVFEM. *Int J Circ Theor Appl.*, *2021;15(2):1-15*.